Efficient Distraction Detection in Surveillance Video using Approximate Counting over Decomposed Micro-streams

Avi Bleiweiss
BShalem Research, Sunnyvale, U.S.A.

Keywords: Stream Data, Approximate Counting, Sliding Window, Cosine Distance, Surveillance Video, Classification.

Abstract: Mining techniques of infinite data streams often store synoptic information about the most recently observed data elements. Motivated by space efficient solutions, our work exploits approximate counting over a fixed-size sliding window to detect distraction events in video. We propose a model that transforms inline the incoming video sequence to an orthogonal set of thousands of binary micro-streams, and for each of the bit streams we estimate at every timestamp the count of number-of-ones in a preceding sub-window interval. On window bound frames, we further extract a compact feature representation of a bag of count-of-1's occurrences to facilitate effective query of transitive similarity samples. Despite its simplicity, our prototype demonstrates robust knowledge discovery to support the intuition of a context-neutral window summary. To evaluate our system, we use real-world scenarios from a video surveillance online-repository.

1 INTRODUCTION

Instinctive discovery of a context shift in streaming large volumes of video sequences is a widely studied problem that has attracted extensive research for the past dozen years. Change detection is one of principal interests to diverse real-time application domains, including monitoring surveillance feeds, predicting live weather, tracking stock market fluctuations, and relieving network traffic congestion. Despite its scale and practical appeal, abnormal event recognition in a stream remains challenging, as data that arrived before a change can bias the model towards unsubstantiated characteristics that no longer hold.

Time-varying data streams are of a transient nature and often presented online in a prohibitively large size. Retaining the entirety of their underpinned data in an active storage, hence becomes infeasible, and unless stream elements are processed instantly or stored, they are disposed of and presumed unaccessible. Typically, a stream data model allocates a working space of sufficiently limited capacity for placing summaries or parts of streams, to facilitate fast responses in processing continuous queries (Leskovec et al., 2014). One prevalent approach for stream summarization attaches more significance to recent elements relative to those entered at a long time past, and identifies a sliding window of elements arrived between the current timestamp and some recent time formerly. To considerably further reduce the memory footprint required to keep window summaries, our work explores the concept of maintaining approximate counts in streaming data (Datar et al., 2002; Arasu and Manku, 2004; Lee and Ting, 2006). Distinctly, we chose the primitive counting algorithm, DGIM (Datar et al., 2002), that maintains a time-based histogram of active 1's over a bit stream window, partitioned into exponentially increasing bucket sizes. A bucket represents a contiguous time interval and is efficiently described by the timestamp of its most recent end, and the number of ones rendered in the prescribed period. Bucket creation rules are tailored to trade-off between histogram space requirements and the allowable fractional error that transpires in computing approximate counts.

To the best of our knowledge based on published research to date, our framework is the first to incorporate anytime query of approximate element counts, for telling apart a disruptive event in a sustained video stream. We operate simultaneously on many thousands of factorizable binary micro-streams that are created inline, and abide by a uniform arrival data-rate and a consistent time interval between elements. As each micro-stream temporally links inbound frame pixels of a spatially identical, two-dimensional coordinate set. At every window frame boundary, we further coalesce individual micro-stream summaries into an extremely compact representation of a bag of

Bleiweiss, A.
Efficient Distraction Detection in Surveillance Video using Approximate Counting over Decomposed Micro-streams.
DOI: 10.5220/0006067103270335
In *Proceedings of the 8th International Joint Conference on Knowledge Discovery, Knowledge Engineering and Knowledge Management (IC3K 2016) - Volume 1: KDIR*, pages 327-335
ISBN: 978-989-758-203-5

count-of-1's occurrences. Our work closely leverages information retrieval (IR) practices, letting window feature vectors perceived as directions (Baeza-Yates and Ribeiro-Neto, 1999) that follow efficient cosine similarity calculations, directly from the well known Vector Space Model (Salton et al., 1975).

The main contribution of our work is a high-performance software prototype that devises to keep an exceptionally compressed rendition of a window summary. Our learning model is able to make more informed decisions by classifying distractions over potentially a cascade of many retained instances of past windows, as it gains from expanding on the single window visibility that reasons similarity in the time span defined between the current and previous windows. Furthermore, to conform to real-time query responses as new video frames arrive, our system is designed to update bucket properties of all micro-streams concurrently. Thus efficiently subscribing to the processing step implied by the requisite of satisfying DGIM bucket terms, evidently the most intensive compute task in our pipeline. To evaluate our framework, we use real-world datasets obtained from the Video Surveillance Online Repository (ViSOR) (Vezanni and Cucchiara, 2010; ViSOR, 2010).

2 APPROXIMATE COUNTING

In this section, we briefly overview the DGIM algorithm (Datar et al., 2002) as it pertains to a single binary micro-stream. At its core, the sliding window model continuously maintains active statistics over the recently observed N data elements of the stream, as each element expires after exactly N time steps. An element is identified by an absolute frame arrival-time, and has a timestamp that corresponds to its relative position in a window. The DGIM method uses an effective histogram data structure to represent a window, and provides at anytime a response time of $O(1)$ for querying the estimated count of ones in the most recent k bits, for any $1 \leq k \leq N$. A histogram bucket, b, is defined by both the timestamp modulo N of its most recent one arrived, t_s, and the count of ones it contains, denoted henceforth as the bucket size, $|b|$, that must be a power-of-2 number. Storage wise, to retain a bucket we need $\log_2 N$ bits for the timestamp and $\log_2 \log_2 N$ bits for the size, thus a memory area of $O(\log N)$ bits suffices. On the other hand, there are at most two buckets of all sizes from $\log_2 N$ down to one, and no buckets of larger sizes. With $O(\log N)$ buckets, each of $O(\log N)$ bits, the total space required for all the buckets representing a window of size N elements is therefore $O(\log^2 N)$ bits.

time	25	40	47	52	55	58	60	61	62	63	64	65
timestamp	25	0	7	12	15	18	20	21	22	23	24	25
bucket size distribution	8	8	4	2	2	1	1					
	8	8	4		4		2	1				
	8	8	4		4		2	1	1			
	8	8	4		4		2		2	1		
	8	8	4		4		2		2	1	1	
		8			8				4		2	1

Figure 1: Satisfying DGIM rules: showing both arrival-time and timestamp for a window of $N = 40$ bits. Current time is 60, and at positions 61 through 65, a series of 1's appear in the stream. Bucket size adaptation often involves the merger of two adjacent buckets of the same size into one bucket of twice the size. The timestamp of the new bucket is the more recent of the bucket pair.

A guiding principle in constructing the bucket representation of a stream window as a series of $(t_s, |b|)$ pairs, states that every position with a one must be in some bucket, but in no more than a single bucket. As a new bit element arrives, we follow these steps to modify the histogram and satisfy the DGIM rules:

- First, we check the earliest bucket. If its timestamp reached $N+1$, the bucket has expired and dropped from the list.
- No change is required for a new data element of 0. Otherwise, we create a new bucket with the current timestamp and a size of one.
- We then traverse the bucket list in a non-decreasing size order. If there are more than two buckets of the same size, we merge the earliest pair of buckets into a single bucket of twice the size, and its timestamp set to the more recent of the two buckets.

The last step may unfold into a chain of bucket merges, limited however to at most $\log_2 N$ unique bucket sizes. Figure 1 further illustrates bucket size adaptation in a real-world scenario, as new bits appear in the stream. Respectively, at time 65, bucket $(25, 8)$ falls out of the window and is thereby dropped. As three buckets of size one are formed, we combine the leftmost two, $(24, 1)$ and $(23, 1)$, and replace them with bucket $(24, 2)$. This leads to three buckets of size two, thus merging $(22, 2)$ and $(20, 2)$ into $(22, 4)$. Consequently, three buckets of size 4 arise and we unite $(15, 4)$ and $(7, 4)$ to create $(15, 8)$. Merging two adjacent buckets of identical size requires constant time and hence, a new data bit can be efficiently processed in $O(\log N)$.

At any time step, to produce an estimate of the count of active ones in the last k bits of the window, for some $1 \leq k \leq N$, we locate the bucket with the earliest timestamp that includes at least some of the k most recent bits. The approximate count of ones becomes the sum of the sizes of all the succeeding buckets, plus half the size of the earliest bucket. The absolute error, ε, in this estimate is hence no greater than 50% of the earliest bucket size. By increasing the number of buckets, r, for each size ($r > 2$), we introduce more buckets of smaller size and the error is therefore upper bounded by $1/(r-1)$. This property is essential and implies that choosing sufficiently large r limits the error to any suitable fraction $\varepsilon > 0$.

3 DISTRACTION DETECTION

Before we detail the steps to learn counting features in a self-sustained time-series, we introduce some notation. The incoming frame-based video is best interpreted in our system as a macro-stream represented by a matrix S of separable binary micro-streams, each proceeding along the time course of a respective frame pixel. Given the uniform frame extent of width n and height m, the total number of micro-streams our system maintains and queries simultaneously for approximate counts is hence $n \times m$. Spatially, we denote a temporal micro-stream, s_{ij}, where $1 \leq i \leq m$ and $1 \leq j \leq n$ (Figure 2). Correspondingly, we define a count matrix, C_w, we sample at successive window-bound frames $\in \{N, 2N, ..., WN\}$, where W is the maximum admissible integral number of windows delimited by the length, in frames, of the input video sequence, as w takes running window indices $\in \{1, 2, ..., W\}$. Elements c_{ij} of the count matrix, capture the estimate of count of ones in the k frames preceding the current window boundary, for each binary micro-stream, respectively. Incidents of identical counts in C_w, each in the $[0,k]$ range, are summed and further binned into a compact bag of words vector, V_w, of a reduced dimensionality $|V_w| = k+1$. V_w is of linear $O(k)$ storage and provides for both efficient similarity computations, and for retaining an extended past of window summaries.

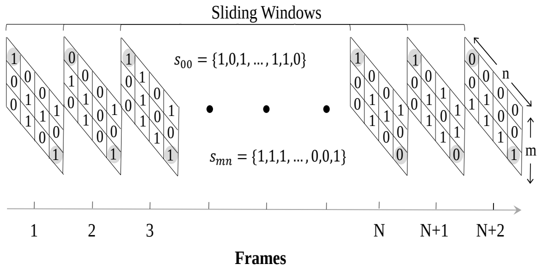
Sliding Windows
$s_{00} = \{1,0,1,...,1,1,0\}$
$s_{mn} = \{1,1,1,...,0,0,1\}$
n
m
1
2
3
N
N+1
N+2
Frames

Figure 2: Sliding window visualization of the incoming binary converted macro-stream, highlighting the time course expansion of bits for micro-streams s_{00} and s_{mn}.

Our process for analyzing distraction events in a macro-stream, commences with the extraction of window bound features, as outlined in Algorithm 1. Every video frame that enters our pipeline is first binary converted from a gray-scale or color format by constructing the frame intensity histogram and applying pixel-level thresholding. A newly arrived frame is timestamped modulo N, and is thereafter interpreted as an m by n array of new bits, each corresponding to the spatially matching micro-stream, s_{ij}. At its outset, the baseline of a new frame launches a concurrent bucket update for maintaining the DGIM rules, and affects the entire collection of micro-streams, s_{ij}. We determine a window boundary, after an initial latency of N frames and for every N frames that follow, by testing timestamp modulo N for zero. At window markers, we query the estimated count of ones for the past k frames from each micro-stream, s_{ij}, and respectively fill the cells, c_{ij}, of our window specific count matrix, C_w, simultaneously. Lastly, we perform a reduction operation on the current count matrix that leads to our compressed window feature vector, V_w. The number of active past windows, W, for retaining window feature vectors, prescribes a fixed time interval to learn distractions from, and is either derived directly, or set as a not-to-exceed system level parameter for an infinite video sequence.

Algorithm 1: Window Feature Extraction.

```
 1: input: frame $f$, window $N$, frames-of-interest $k$
 2: output: window feature vector $V \leftarrow \emptyset$
 3: $timestamp \leftarrow index(f) \bmod N$

 4: for $i = 1$ to $m$ do
 5:    for $j = 1$ to $n$ do
 6:       $update\text{-}bucket(s_{ij}, threshold(f_{ij}))$
 7:       if not$(timestamp)$ then
 8:          $c_{ij} \leftarrow query(s_{ij}, k)$
 9:       end if
10:    end for
11: end for
12: if not$(timestamp)$ then
13:    $V \leftarrow bag\text{-}of\text{-}counts(C)$
14: end if
15: return $V$
```

For detecting distraction, we match features of the sampled windows at integral multiples of N frames, by computing a single-term form of similarity between the pair of the current and previous window representations. Our window properties are inherently directional and are distributed in a non-Euclidean space, hence we chose cosine similarity (Salton et al., 1975; Baeza-Yates and Ribeiro-Neto,

1999) as the distance metric that measures the angle between the two window-bound feature vectors

$$sim_w = \frac{V_w \cdot V_{w-1}}{\| V_w \|_2 \| V_{w-1} \|_2}, \qquad (1)$$

where w is the running index of the current window, such that $w \geq 2$. In addition to the window feature vector, V_w, we also retain the point similarity measure, sim_w, that requires $O(1)$ storage space, per window. In its basic embodiment, our system alerts a distraction event on a window edge, as the point similarity value computed exceeds a globally specified threshold parameter, τ. Conversely, by maintaining a series of distances for formerly evaluated window pairings, we fit discretized similarity samples of multiple past windows onto a curve. We could then use a more generalized version of the dynamic time warping algorithm (Efrat et al., 2007), for matching a pair of partially overlapping similarity curves, each comprised of an identical distance sample-count.

4 EVALUATION

To evaluate our system in practice, we have implemented a software prototype that realizes the concept of maintaining stream statistics over sliding windows, for effective distraction detection. A distraction marks an abrupt shift in a stable context that typifies the input stream, and may last up to a few seconds. We use OpenCV to capture real-world surveillance video and feed each frame to our processing pipeline, designed with the objective to keep up with incoming frame rate. For conciseness, we use the compact notation $\lambda(N,k)$ to describe our parametrically driven implementation, and seek to analyze the impact of varying model parameters on our system performance.

4.1 Experimental Setup

One indispensable resource for practitioners in the field of analyzing surveillance video is the publicly accessible, Video Surveillance Online Repository (ViSOR) (ViSOR, 2010). ViSOR is highly extensive and offers over a dozen of surveillance datasets acquired by tracking both indoor and outdoor environments for many hours, and captured by either static or dynamic settings of single and multi camera installations. The video sequence footage produced is available in either a compressed or an uncompressed format, and may optionally contain companion annotation meta-data (Vezanni and Cucchiara, 2010) for use as a ground-truth reference. In our experiments, we employed three surveillance streams from the ViSOR dataset of the Unimore university that surveyed the near outdoors of several campus buildings. The properties of the sequences, we henceforth denote as visor_i, where $i \in \{1,2,3\}$, are further listed in Table 1. Our experimental videos are natively MPEG-1 compressed, they share a uniform frame resolution that translates to 98,304 micro-streams for each, and frames are presented in a single-component grayscale format. The filed length of the videos varies from over two to about seventeen thousand frames, and facilitates a reasonable sampling rate for learning window bound features.

Table 1: Properties of the three ViSOR surveillance sequences we use in our experiments. They track the near outdoors of a confined Unimore campus area by deploying a multi camera setup.

			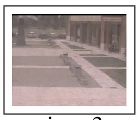
	visor_1	visor_2	visor_3
Width	384	384	384
Height	256	256	256
Frames	2631	8661	17078
FPS	25	25	25

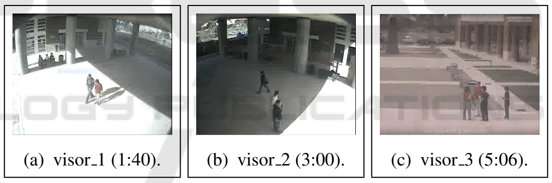
(a) visor_1 (1:40). (b) visor_2 (3:00). (c) visor_3 (5:06).

Figure 3: Distraction snapshots of people entering the field-of-view of the static camera, shown for each of the ViSOR sequences (in minutes into the video from start).

Our experimental videos track a fairly benign and mostly static background (Table 1), as one or several persons walk or rush their way and occasionally enter and thereafter exit the camera field-of-view, to establish a scene distraction (Figure 3). ViSOR test streams are supplemented by concept data that is rather abstract, and to serve a useful ground-truth in our evaluation required us to manually assemble pertinent timing information. We have thus extended the ViSOR meta-data by hand annotating occurrences of distraction, linking each record to a scene in-and-out time-interval. Intervals are inherently non-overlapping and their endpoints assigned absolute frame timestamps. From our ViSOR videos, we singled out 14, 7, and 44 events of interest, respectively, along with their distinct intervals (see APPENDIX).

Our experiments ascribe a discrete value set to each of our model parameters, N and k, listed in Ta-

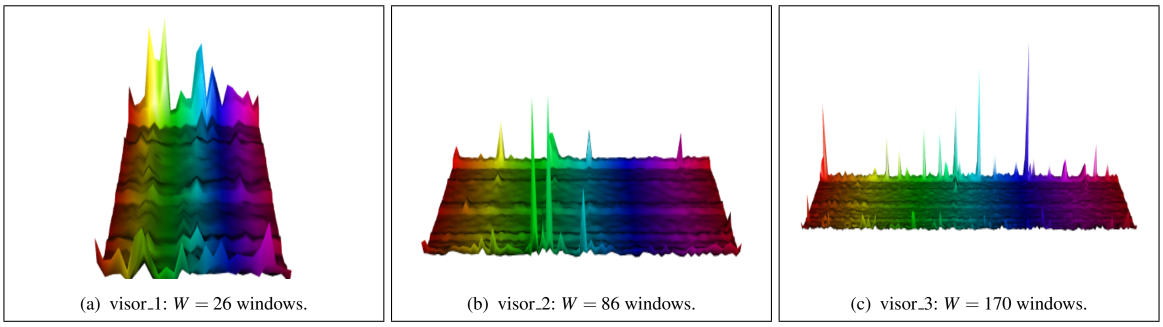
(a) visor_1: $W = 26$ windows. (b) visor_2: $W = 86$ windows. (c) visor_3: $W = 170$ windows.

Figure 4: Visualization of temporally distributed, window-bound feature vectors, V_w, extracted for stream counting parameters $N = 100$ and $k = 50$. Presented as a height field over a two-dimensional grid, $(W, k+1)$, and shown for each of our ViSOR experimental sequences.

Table 2: Experimental parameter selection of window size, N, in frames, and k, the number of past frames, or prior bits in the context of a micro-stream, to query an approximate count of ones.

Window (N)	Query (k)		
100	10	20	50
200	20	50	100
500	50	100	250

ble 2. For each window length choice, N, there are three query period selections, k, that range proportionally between 10 to 50 percent of the window size. Ultimately, we seek the proper design trade-offs in choosing both intra and inter window parameter pairings, to improve the system success rate for detecting distraction. For the current implementation, we present results pertained to our point based similarity approach, however, extending to similarity curve matching (Efrat et al., 2007) is outside the scope of this study and is deferred to future work.

4.2 Experimental Results

In a system of similar goals as ours, exercising overly conservative and more cautious practices is often devised for signaling a distraction event in a stream. The percentage of false positives we encounter is directly related to the choice of our similarity threshold value, τ, thus subscribing to more unintentional event triggers with a lower τ. To properly adapt to action choices taken upon alert, we made similarity threshold setting a user tunable. On the other hand, attending to false negatives and sustain a reduced miss rate is of a taller order in our design. False negatives are primarily impacted by the error bound to the approximate count of ones we solicit from a micro-stream, and is inversely proportional to the number of occurrences set for the same bucket size, r. For our experiments, we configured the construction of the time histograms with $r = 2$, to yield a worst-case counting error, and report next results that score both the identifying and misinterpreting distraction events in our ViSOR samples.

First, we validated the temporal evolution of our approximate count features in a macro-stream. A surface visualization of the extracted window vectors, V_w, is shown for each of the three ViSOR sequences, with $W = \{26, 86, 170\}$ progressive windows, respectively, as model parameters, (N, k), are assigned uniformly to $(100, 50)$ (Figure 4). The height field is rendered over a two-dimensional regular grid, $(W, k+1)$, and cells depict each a scaled count value, aligned with elements of the unnormalized feature vectors.

Rather than explore post-threshold results that are notably less informative, we present unsolicited point similarities. Given the non-negative elements of our bag-of-counts window features, V_w, the cosine similarity term produces a value bound to the $[0, 1]$ range. To improve clarity of our reporting, we resort to the more intuitive metric of cosine distance instead, that attributes greater distraction, or dissimilarity, to a higher value. For every ViSOR surveillance video, Table 3 outlines a curve of point dissimilarities, each for a pair of window feature vectors, (V_w, V_{w-1}), as a function of an ascending window id, and factored by our test choices of model parameters, (N, k). Along with Table 4 that provides a complementary matrix form for summarizing the number of identified incidents obtained from each stream, as a function of our model parameter choices. Predicted distraction instances are further correlated with our hand annotated, ground-truth interval data. Every interval represents a double-edged incident, with distractions occurring upon entry to and exit from the camera field-of-view, respectively. An interval either overlaps two or more windows, a form that fits well our current-to-previous count matching model, or may entirely be confined to a single window and occasionally give rise to missing events. To properly account for precedence of false negatives, we chose the F1-score metric to assess our system-level distraction detection, as out-

Table 3: Curve outline of point dissimilarities, each for a pair of window feature vectors, (V_w, V_{w-1}), as a function of an increasing window id. Factored by each of our experimental choices of model parameters, (N, k), and shown for each ViSOR surveillance video.

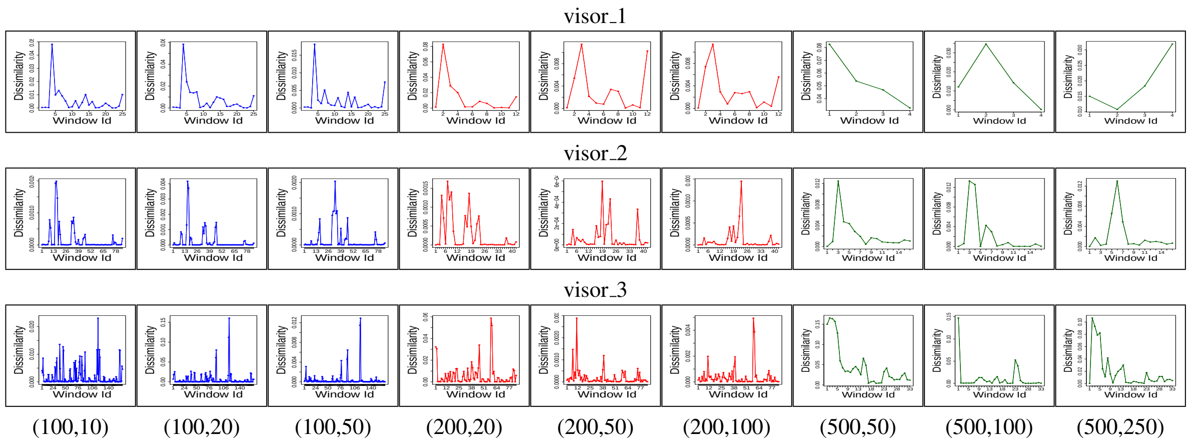

Table 4: Distraction occurrence prediction shown as 3x3 matrices for our N by k choices (Table 2), for each of the ViSOR sequences.

N	visor_1			visor_2			visor_3		
100	15	13	15	24	24	18	67	54	34
200	7	8	9	18	20	16	51	47	48
500	3	2	2	9	10	8	18	13	16

lined in Table 5 for each of the ViSOR videos. For reference, Table 6 provides confusion matrices for each of our videos, as we set false positives uniformly to zero since they incur little impact on system performance. Evidently, the end-to-end F1-score improves as the stream length increases, and not surprisingly, both a narrower N for denser sampling of window features, and a smaller k for the more recent frames used to query counts, ameliorate our anomaly hit rate.

Table 5: F1-score measure for system-level distraction detection, for each of the ViSOR video sequences.

visor_1	visor_2	visor_3
0.69	0.73	0.86

Table 6: Confusion matrices of two-class classification for stream counting parameters $N = 100$ and $k = 10$, for each of the ViSOR video sequences.

	visor_1	
Real	15	13
	0	12
	Predicted	

	visor_2	
Real	14	10
	0	73
	Predicted	

	visor_3	
Real	67	21
	0	83
	Predicted	

Our system provides for comparing performance of our pixel-based time histogram with a more baseline approach of a frame-based intensity histogram. For this experiment, we retained a window-worth of intensity histograms that we construct every frame right before performing binary thresholding. We considered 256 bins and computed the mean of the histograms over a window of N frames to extract a window feature vector of cardinality $|V_w| = 256$. Notably for the baseline method, we observed an appreciable increase of false negatives by about 43% on average across our ViSOR videos. Incurring this higher miss rate owes primarily to a suboptimal baseline representation that severely compromises the stream data. Rather, our approach decomposes a video into many thousands of signals processed individually, to closely preserve the integrity of the original macro-stream and thus facilitates more robust discovery of distraction patterns. Computationally, our method with time complexity $O(mn \log N)$ naturally entails more load when executed serially, however, a parallel GPU concept that assigns a thread to each of the micro-streams is capable of a markedly $O(\log N)$ lower bound.

Table 7: Average frame rate (FPS) and average micro-stream processing (uSP) time in microseconds as a function of modified model parameters, (N, k), for each of our experimental ViSOR video streams.

		visor_1		visor_2		visor_3	
N	k	FPS	uSP	FPS	uSP	FPS	uSP
100	10	12.57	0.72	16.51	0.55	11.48	0.79
	20	11.23	0.81	18.31	0.49	12.06	0.75
	50	10.86	0.83	19.34	0.47	12.73	0.71
200	20	10.85	0.83	14.98	0.60	11.23	0.81
	50	10.17	0.89	18.04	0.50	11.01	0.82
	100	10.38	0.87	18.47	0.49	11.49	0.79
500	50	10.40	0.87	14.16	0.64	10.00	0.90
	100	9.31	0.97	17.56	0.51	9.17	0.99
	250	9.30	0.97	17.60	0.51	9.18	0.98

In Table 7, we provide computational runtime of our implementation, listing for each of the experimental ViSOR videos the average of both the frame rate

Table 8: A distraction event in the visor_3 video that arises as a result of a moving white vehicle (outlined in red) that traverses the camera field-of-view from right to left in about a second and totals 25 frames of exposure. The event interval starts at about frame number 5322 and shown are samples captured on three-frame successions.

5325	5328	5331	5334	5337
		frame number		

(FPS) and micro-stream processing (uSP) time, measured in microseconds, as we alter our model parameters, (N,k). There is a clear monotonic decrease in performance as we increase the window size, N, at a rate that is close to the ratio $\log N_{i-1}/\log N_i$, where i associates with the current window-size setting. However, the runtime depends rather weakly on the model parameter k, as both the check for bucket expiration and the query of approximate counting are processed efficiently. We demonstrate the highest performance on visor_2, and this is mainly attributed to its fairly sparse and temporally low distraction density of 1250 frames-per-event (FPE) on average, compared to an FPE of 188 and 38 for visor_1 and visor_3, respectively. Noteworthy in this report is the observed quadratic impact of the surveillance camera resolution on our running time. To further address high definition video, our implementation is capable of tasking groups of micro-streams concurrently and sustain a required real-time response for notifying distraction occurrences as they continuously develop.

Distraction events in our ViSOR test sequences are mostly typified by the motion of humans (Figure 3). However, they also occasionally manifest themselves by vehicle passing that transpires in the somewhat far background of the monitored area. Figure 8 depicts such a scenario in the visor_3 video where a white vehicle moves across the camera field-of-view right-to-left and thereof constitutes a valid distraction instance. This event starts at around frame number 5322 and lasts about a second for a total exposure of 25 frames, with samples shown for every third frame. Vehicular based events either occur autonomously or may coincide with a human triggered event. Semantically, our system interprets both event types equally and makes no attempt to distinguish between them in processing a distraction alert. We avoided hand-annotating vehicular episodes in the meta-data of our experimental videos, and unless a human distraction occurrence overlaps with a vehicular one, the event is presumed false positive.

5 RELATED WORK

Over the past decade, a wide range of diverse schemes were proposed for automating abnormal event detection in surveillance videos. Among some of the many algorithms considered in published literature are techniques that incorporate optical flow, including a Markov Random Field model that divides the video into a graphically linked grid of spatio-temporal local regions to facilitate probabilistic motion patterns (Jaechul and Grauman, 2009), and the more recent research that analyzes compressed domains by consulting codec-dependent meta-data to provide more accurate object boundaries (Li et al., 2014). To address complex events, Chen *et. al* (2015) proposed a hypergraph based semi-supervised learning method that blends motion features with semantic concepts. Compared to techniques that deploy ordinary graphs, they report better average precision and recall for detecting multiple moving targets. More data driven is the spectral clustering method that utilizes an eigenvector selection to discover natural grouping patterns (Xiang and Gong, 2008). Whereas a device specific work by Shimada *et. al* (2015), embodies a stream originated by a light-field camera to create and update a light-ray background model that changes dynamically, and demonstrates advantage over a single-view camera. At a higher level of abstraction, Lee and Nevatia (2014) sought after a tool that uses shape based approach to validate whether an identified abnormal event was triggered by a human or not.

Most of the techniques discussed for detecting change in an infinite stream tend to build explicit and often oversubscribed models to associate with many normal events, thus making a distraction hard to define. Our work rather compares a current event with the rest of the events observed (Zhong et al., 2004), and furthermore, by rendering the video as a collection of opaque bit streams, it makes no prior behavioral assumptions and neither subscribes to visual context dependencies.

6 CONCLUSIONS

We have demonstrated the apparent potential in tailoring approximate counting to effectively detect distractions in unbound surveillance videos, with little human counseling. Our highly compact bag-of-counts representation is scalable and provides learning of many windows that outline a deeper past, to facilitate the expansion of the more conventional, point similarity approach. Running on an unoptimized prototype version, the obtained sustainable throughput of about half the input frame-rate on average, consistently on all of our experimental videos and the full extent of model parameter settings, provides for real-time application compliance.

A natural progression of our work is to reduce the absolute counting error by introducing more smaller buckets for constructing the time-based histogram over a window, and improve overall detection rate. Rather than a step function that characterizes window transitions in the current implementation, the use of a tapered sliding window offers overlapping windows, as frames gradually enter and exit the window, to further assist and lower distraction misses.

ACKNOWLEDGEMENTS

We would like to thank the anonymous reviewers for their insightful suggestions and feedback.

REFERENCES

Arasu, A. and Manku, G. S. (2004). Approximate counts and quantiles over sliding windows. In *Principles of Database Systems (PODS)*, pages 286–296, Paris, France.

Baeza-Yates, R. and Ribeiro-Neto, B., editors (1999). *Modern Information Retrieval*. ACM Press Series/Addison Wesley, Essex, UK.

Chen, X. J., Zhan, Y. Z., Ke, J., and Chen, X. B. (2015). Complex video event detection via pairwise fusion of trajectory and multi-label hypergraphs. *Multimedia Tools and Applications*, pages 1–22.

Datar, M., Gionis, A., Indyk, P., and Motwani, R. (2002). Maintaining stream statistics over sliding windows. *SIAM Journal of Computing*, 31(6):1794–1813.

Efrat, A., Fan, Q., and Venkatasubramanian, S. (2007). Curve matching, time warping, and light fields: New algorithms for computing similarity between curves. *Mathematical Imaging and Vision*, 27(3):203–216.

Jaechul, K. and Grauman, K. (2009). Observe locally, infer globally: A space-time MRF for detecting abnormal activities with incremental updates. In *Computer Vision and Pattern Recognition (CVPR)*, pages 2921–2928, Miami, FL.

Lee, L. K. and Ting, H. F. (2006). Maintaining significant stream statistics over sliding windows. In *Discrete Algorithm (SODA)*, pages 724–732, Miami, FL.

Lee, S. C. and Nevatia, R. (2014). Hierarchical abnormal event detection by real time and semi-real time multi-tasking video surveillance system. *Machine Vision and Applications*, 25(1):133–143.

Leskovec, J., Rajaraman, A., and Ullman, J. D., editors (2014). *Mining of Massive Datasets*. Cambridge University Press, New York, NY.

Li, H., Zhang, Y., Yang, M., Men, Y., and Chao, H. (2014). A rapid abnormal event detection method for surveillance video based on a novel feature in compressed domain of HEVC. In *Multimedia and Expo (ICME)*, pages 1–6, Chengdu, China.

Salton, G., Wong, A., and Yang, C. S. (1975). A vector space model for automatic indexing. *Communications of the ACM*, 18(11):613–620.

Shimada, A., Nagahara, H., and Taniguchi, R. I. (2015). Change detection on light field for active video surveillance. In *Advanced Video and Signal Based Surveillance (AVSS)*, pages 1–6, Karlsruhe, Germany.

Vezanni, R. and Cucchiara, R. (2010). Video surveillance online repository (ViSOR): an integrated framework. *Journal of Multimedia Tools and Applications*, 50(2):359–380.

ViSOR (2010). Video surveillance online repository. http://www.openvisor.org .

Xiang, T. and Gong, S. (2008). Video behavior profiling for anomaly detection. *Pattern Analysis and Machine Intelligence*, 30(5):893–908.

Zhong, H., Shi, J., and Visontai, M. (2004). Detecting unusual activity in video. In *Computer Vision and Pattern Recognition (CVPR)*, pages 819–826, Washington, DC.

APPENDIX

Our meta-data for hand annotated time intervals that capture distraction instances from each of our ViSOR sequences are listed in Table 9.

Table 9: Hand annotated, in-and-out time intervals that capture distraction events from each of our ViSOR sequences. Interval endpoints and duration are shown in a minutes:seconds format, as intervals extend to either wholly or partially cover one up to four windows.

visor_1

event	in	out	duration
1	0:02	0:03	0:01
2	0:18	0:20	0:02
3	0:27	0:28	0:01
4	0:29	0:30	0:01
5	0:40	0:42	0:02
6	0:45	0:47	0:02
7	0:49	0:50	0:01
8	0:51	0:55	0:04
9	0:58	1:02	0:04
10	1:04	1:07	0:03
11	1:17	1:18	0:01
12	1:33	1:35	0:02
13	1:36	1:37	0:01
14	1:40	1:41	0:01

visor_2

event	in	out	duration
1	0:04	0:05	0:01
2	0:55	1:00	0:05
3	1:03	1:06	0:03
4	2:01	2:03	0:02
5	2:10	2:12	0:02
6	2:17	2:20	0:03
7	2:54	3:02	0:08

visor_3

event	in	out	duration
1	0:02	0:03	0:01
2	0:07	0:09	0:02
3	0:17	0:20	0:03
4	0:55	1:01	0:06
5	1:29	1:30	0:01
6	1:51	1:53	0:02
7	1:59	2:06	0:07
8	2:16	2:19	0:03
9	2:29	2:35	0:06
10	3:00	3:03	0:03
11	3:18	3:21	0:03
12	3:48	3:51	0:03
13	3:57	3:59	0:02
14	4:10	4:13	0:03
15	4:27	4:31	0:04
16	4:32	4:34	0:02
17	4:42	4:46	0:04
18	4:49	4:51	0:02
19	4:59	5:02	0:03
20	5:05	5:14	0:09
21	5:38	5:40	0:02
22	5:44	5:47	0:03
23	5:54	5:56	0:02
24	5:59	6:02	0:03
25	6:20	6:23	0:03
26	6:38	6:45	0:07
27	6:49	6:52	0:03
28	7:01	7:04	0:03
29	7:08	7:11	0:03
30	7:24	7:25	0:01
31	7:28	7:31	0:03
32	7:44	7:45	0:01
33	7:47	7:50	0:03
34	7:57	8:00	0:03
35	8:04	8:05	0:01
36	8:07	8:10	0:02
37	8:22	8:24	0:02
38	9:16	9:21	0:05
39	9:53	10:03	0:10
40	10:08	10:11	0:03
41	10:26	10:31	0:05
42	10:54	10:57	0:03
43	10:58	11:00	0:02
44	11:13	11:16	0:03